Fast Orange Peel-Mediated Synthesis of Silver Nanoparticles and Use as Visual Colorimetric Sensor in the Selective Detection of Mercury(II) Ions

Abdulmalik Aminu[1] · Sulayman A. Oladepo[1]

Abstract

This paper presents the green synthesis of silver nanoparticles (AgNPs) using orange (*Citrus sinensis*) peel extract. The effects of different factors such as silver ion concentration, reaction time, temperature, pH, and extract quantity on the AgNPs synthesis were studied, enabling us to determine optimum synthesis conditions. We characterized the AgNPs with different techniques: UV–Visible Spectroscopy, Field Emission Scanning Electron Microscopy (FESEM), FTIR, and XRD. The AgNPs showed yellowish brown to golden brown colors and a surface plasmon resonance (SPR) absorption band around a wavelength of 420 nm. FESEM images showed polydisperse AgNPs having an average size of about 55 nm. The XRD profile of the synthesized nanoparticles showed peaks that are characteristic of silver while the FTIR spectrum highlighted the functional groups associated with reducing silver ions and stabilizing the AgNPs. With the selected optimum conditions, the AgNPs were formed in less than 1 min. This is the fastest reaction time so far reported and is significantly shorter than in earlier reports. The AgNPs colloid solution was applied as nanosensor in the visual colorimetric detection of mercury(II) ions in water. The golden brown AgNPs colloid solution turned colorless and the characteristic SPR absorption band disappeared when mercury(II) ions were added to the solution. While the AgNPs show good sensitivity and selectivity for the colorimetric detection of mercury(II) ions with a detection limit of 1.24×10^{-6} mol/L (0.25 ppm), we also demonstrated the suitability of the method for detecting mercury(II) ions in drinking water.

Keywords Silver nanoparticles · Fast AgNPs synthesis · Colorimetric Hg^{2+} detection · SPR absorption band · Green AgNPs synthesis

1 Introduction

Silver nanoparticles (AgNPs) are a class of noble metal nanoparticles that have attracted research attention due to their dynamic properties and vast areas of applications. These nanoparticles possess the capability to strongly absorb electromagnetic waves in the visible region, they possess favorable optical and electrochemical properties and they also show good biological compatibility and high extinction coefficient [1–3]. Such properties allow their utilization in medical, bioimaging, and biosensing applications [4]. The incorporation of nanomaterials into sensing systems is advantageous in the area of molecular sensing, as they offer better stability, enhanced sensitivity, and improved cost-effectiveness [5]. Orange (*Citrus sinensis*) peel is the protective layer of an orange fruit which is made up of an albedo (inner layer) and a flavedo (outer layer). The peel biomass possesses high amounts of natural antioxidants like flavonoids, resins, monoterpenes, phenols, carotenoids, and saponins which makes it suitable for certain medicinal and chemical uses, one of which is as reducing agents in the green synthesis of AgNPs [6]. Generally, plants represents a good and easily available source of bioactive species such as polysaccharides, proteins, polyphenols, flavonoids, alkaloids, amines, ketones, aldehydes, terpenoids, and tannins, which act as reducing, stabilizing and capping agents in the formation of nanoparticles [7].

✉ Sulayman A. Oladepo
  saoladepo@kfupm.edu.sa

1 Department of Chemistry, King Fahd University of Petroleum and Minerals, Dhahran 31261, Kingdom of Saudi Arabia

Routine physical and chemical methods of synthesizing nanoparticles can be energy and capital intensive, while they employ toxic chemicals and non-polar solvents, which preclude their use in clinical and biomedical applications [8]. This warrants the development of clean, biocompatible and benign synthetic methods. In addition, sustainability awareness and concerns also contribute to the need for simple, reliable, and eco-friendly (green) method of synthesizing nanoparticles [8, 9]. Several authors have presented comprehensive lists of various plant extracts used for the synthesis of metal nanoparticles [8–10]. Such green synthetic routes are devoid of complex and multi-step procedures, and so are comparatively very simple, fast, and cost-effective [8], thereby, making their exploration and adoption attractive. Interestingly, water is the main environmentally friendly solvent used for green nanoparticle synthesis [9]. Other attractive features of green nanoparticle synthesis include being one-pot reaction, absence of toxic chemicals, being amenable to scale up, and colloidal stability due to the presence of natural products that serve as reducing and capping agents [7–9].

Mercury is characterized as the most potent pollutant among all heavy metals and it poses grave concern globally due to its high persistence in the environment especially in the oceans and seas [11]. Contamination by mercury occurs as a result of natural phenomenon such as volcanic eruptions or from human activities that utilize or produce mercury compounds in mining, chemical, agricultural, and pharmaceutical industries [12]. These processes entail the use of mercury in fungicides, antiseptics, preservatives, and dental amalgams. There are various analytical techniques used in the determination of mercury, prominent among them are the instrumental methods of analysis like cold vapor atomic absorption spectroscopy [13], flame photometry [14], inductively coupled plasma mass spectrometry [15], and solvent extraction followed by high-performance liquid chromatography (HPLC) [16]. These methods provide exceptional performance and high sensitivity but they are quite expensive, complex, and they require intricate sample preparation protocols. Therefore, new analytical methods that may be simpler and cheaper are being explored.

Colorimetry is a well-known analytical technique that is commonly used in routine analysis. As of recent, colorimetric sensors have been explored in the detection of Hg^{2+} and they have been tagged as simple, rapid, sensitive, and highly selective [17, 18]. Some of the methods developed for Hg^{2+} detection utilized fluorophores [19], oligonucleotides and DNA [20, 21], as well as organic compounds [22]. In this context, colorimetry is a widely used method because AgNPs has an absorbance peak in the visible wavelength region around 420 nm due to the surface plasmon resonance (SPR) electrons that reside on the surface of the nanoparticles [7]. The concept of mercury's optical detection by AgNPs involves

the reaction of silver with mercury to form zero-valent mercury, which leads to decolorization of AgNPs colloid solution and the loss of SPR absorption band. This redox reaction occurs between Ag^+/Ag_{nano} ($E^0 < 0.79$ V) and Hg^{2+} ($E^0 = 0.85$ V). The reaction is aided by the unique properties possessed by silver at the nanoscale, which favors the formation of silver–mercury amalgam [17]. Novel nanocomposite and mesoporous materials have also been used extensively for the colorimetric detection, monitoring and removal of mercury(II) as well as other toxic metals. For instance, Awual et al. [23–28] have used such materials extensively and showed that a wide variety of metals can be colorimetrically detected by means of these novel nanocomposite and mesoporous materials. Specifically, for mercury detection their methods show excellent sensitivity and selectivity for the metal ion [23–25].

While all the aforementioned colorimetric methods are successful in providing excellent detection of mercury, several of them involve fairly costly and complex sensor fabrication as well as long detection times [17, 19–28]. Hence, there is a need for simple, fast, and cheap colorimetric detection methods for mercury. In the present work, we have synthesized AgNPs using orange peel extract as reducing agent and we have used the resulting AgNPs colloid solution for a rapid colorimetric detection of mercury(II) ions in water. The use of orange peel extract as reducing agent is expected to yield AgNPs that is non-toxic and stable because of the natural antioxidants present in the extract and the fact that toxic and hazardous chemicals were not involved [7–9]. The novelty of the present work lies in the optimum synthesis conditions that produced the AgNPs in less than 1 min, which is the fastest reaction time so far reported. Thus, the present work is novel in the sense that it presents the fastest synthesis of AgNPs in a record time of 1 min. The protocol reported in this study can be employed by other researchers as a simple, very fast AgNPs synthesis method. Other advantages of the new AgNPs sensor include low cost, one-pot synthesis, non-toxicity, biocompatibility, good selectivity, and colloidal stability. While the detection limit and sensitivity recorded for mercury in the present work is comparable to what have been previously reported [29, 30], they are not as good as the low detection limits that have been reported with nanocomposite and mesoporous sensors and adsorbents [23–25]. Nonetheless, the current work adds to the repertoire of low cost, one-pot, non-toxic AgNPs synthesis methods and it is the fastest so far reported. Also, colorimetric detection of Hg^{2+} with the new AgNPs sensor happens fairly quickly (within 3 min), compared to methods earlier reported that took relatively long times of 5–30 min [23–25, 29]. It should be mentioned that the use of orange peel extract in the current work is an elegant way of putting waste materials to good use and it is consistent with green chemistry and environmental sustainability goals. The unique optical properties of the

nanomaterials product coupled with their stability and selectivity provides a viable opportunity for their use as simple visual colorimetric mercury(II) ion sensors.

2 Experimental

2.1 Chemicals and Solutions

All chemicals and reagents were used as received without further purification. Silver nitrate, $AgNO_3$ (99.8%) was bought from Loba Chemie (India), potassium hydroxide (KOH), and sulfuric acid (H_2SO_4) were procured from Merck (Germany), while potassium bromide (KBr) was obtained from Thermo Fisher (UK). The metal salts used (NaCl, $CaCl_2$, $MgCl_2 \cdot 6H_2O$, $AlCl_3 \cdot 6H_2O$, $Cd(NO_3)_2 \cdot 4H_2O$, $NiCl_2 \cdot 6H_2O$, and $Hg(NO_3) \cdot H_2O$ were all purchased from Sigma Aldrich (USA) or Merck (Germany).

2.2 Preparation of Orange Peel Extract

A fresh orange was purchased from a local store located within King Fahd University of Petroleum and Minerals. The orange was peeled with a clean knife and the peels were cut into small sizes (about $0.5 \times 0.5 \, cm^2$) and washed thoroughly with deionized water. 10 g of the orange peels were boiled in 100 mL of water for 3 min followed by filtration. The extract obtained was then used undiluted in the synthesis of silver nanoparticles.

2.3 AgNPs Synthesis

For the orange peel-mediated synthesis of silver nanoparticles, 40 mL of 0.01 M $AgNO_3$ was mixed with 5 mL of orange peel extract at room temperature and under constant stirring. While 40 mL of the $AgNO_3$ solution was used in all cases, the $AgNO_3$ concentration, extract volume, extract pH, temperature, and reaction time were varied as described in the next section to enable us determine optimum synthesis conditions. In all cases, the reaction progress was visually monitored by observing variations in color of the solution from colorless to yellow to golden brown. A UV–Vis spectrum was taken at the end once the golden brown color has been formed in order to ascertain the formation of silver nanoparticles. Following a systematic study of the various parameters, we established a set of optimum reaction conditions to synthesize AgNPs used for characterization and colorimetric studies. Details of the optimum conditions are presented in Sect. 3.3.

2.4 Study of Physicochemical Parameters

The green synthesis of AgNPs was conducted under varying conditions so as to evaluate the effect of different factors on silver nanoparticles synthesis, size and shape. The effect of silver ion concentration was examined by using 0.01, 0.02, and 0.03 M $AgNO_3$ in the AgNPs synthesis without changing any other parameter. The effect of orange peel extract volume was studied by altering its volume (3 mL, 5 mL, 7 mL, and 10 mL) while keeping other parameters unchanged. Similarly, we also explored the effect of reaction temperature on AgNPs synthesis by carrying out the synthesis at 25 °C, 50 °C, and 75 °C. The impact of pH was studied by varying the pH of the extract in acidic (pH 3, 4, and 5) and alkaline conditions (pH 10, 11, and 12). Finally, we assessed the effect of reaction time in this investigation by studying the UV–Vis absorbance spectra of AgNPs produced after 2, 5, 10, 20, 40, and 80 min of reaction time.

2.5 Characterization of the AgNPs

The knowledge of the physicochemical properties of AgNPs is important as it greatly helps in evaluating their properties and potential applications. Therefore, characterization of AgNPs was conducted in order to assess the functional aspects of the nanoparticles. In this study, the AgNPs prepared were characterized with UV–vis spectroscopy, X-ray diffractometry (XRD), Field emission scanning electron microscopy (FESEM), and Fourier transform infrared spectroscopy (FTIR). We measured the UV–Vis absorbance of the AgNPs colloid solution formed from the synthesis on a dual beam Genesys 10S UV–Visible Spectrophotometer (Thermo Scientific) running on VISION Lite software. For XRD, FESEM, and FTIR characterizations, AgNPs were synthesized in a large 1 L beaker (using the optimum synthesis conditions) and dried in an oven for 18 h. The resulting lumps of AgNPs were carefully broken into powder and used for XRD, FTIR, and FESEM measurements. For FESEM, a small portion of the nanoparticles was placed on aluminum foil followed by coating of the foil's surface with gold before putting the sample into the FESEM instrument. In FTIR, AgNPs were mixed with KBr and the mixture was pelletized. The pellets were used for FTIR measurements.

The X-ray diffraction was carried out using a Rigaku Ultima IV X-ray Diffractometer with a rated tube voltage of 60 kV and 60 mA current running on PDXL integrated X-ray powder diffraction software. Field emission scanning electron microscopy measurements were carried out with a Quattro S FESEM instrument (Thermo Scientific), while FTIR spectra were acquired with a Nicolet 6700 FTIR Spectrophotometer (Thermo Electron Corporation), running on an OMNIC software and the resolution was set to $2.0 \, cm^{-1}$.

2.6 Colorimetric tests

All colorimetric measurements were made at room temperature. In conducting Hg(II) detection using the synthesized

AgNPs, 1 mL aliquot of AgNPs colloid solution was taken and its UV–Vis absorbance spectrum was recorded as blank. In order to establish the sensing propensity of the AgNPs for Hg^{2+} ions, 4 mL of a 1 mM solution of Hg^{2+} was added to 1 mL of AgNPs colloid solution and the resulting solution thoroughly mixed. Various concentrations of Hg^{2+} were also similarly tested by adding of 4 mL of solutions containing different nominal concentrations of Hg^{2+} ions to each 1 mL aliquot of AgNPs in order to determine the sensitivity of the procedure. To investigate the selectivity of the as-synthesized AgNPs in detecting Hg^{2+} ions, 4 mL solutions of cations of representative metals groups; alkali (Na^+), alkali earth (Ca^{2+}, Mg^{2+}, Al^{3+}), and transition (Ni^{2+}, Cd^{2+}) of 1 mM concentration were each added to 1 mL aliquot of AgNPs under same conditions. The changes in color were visually observed and the corresponding absorbance changes were confirmed with the UV–Vis spectrophotometer.

3 Results and Discussion

3.1 Green synthesis of Silver Nanoparticles

Upon the addition of orange peel extract to silver nitrate solutions, a color change was observed from colorless to yellowish brown and to golden brown. The synthesis of AgNPs was monitored by both visual color changes and UV–Vis absorbance measurements. The UV–Vis spectra of the resulting AgNPs showed a broad SPR absorption with a maximum absorbance centered in the 410–440 nm region (Fig. 1). This absorption band is attributable to SPR excitation of silver nanoparticles with sizes ranging from 2 to 100 nm in aqueous medium, and this has been documented in the literature [31].

3.2 Effects of Various Parameters on the Synthesis of Silver Nanoparticles

3.2.1 Effect of Silver Ion Concentration

The effect of $AgNO_3$ concentration on silver nanoparticles is shown in Fig. 1. As the concentration of Ag^+ ions increases, the absorption intensity of AgNPs colloid solution increases. Some literature reports have established a positive relationship between metal ion concentration and the intensity of the absorption peaks [32]. The present study explored the effect of $AgNO_3$ concentration on AgNPs synthesis by using 0.01, 0.02, and 0.03 M $AgNO_3$. For each concentration, the synthesis was carried out at room temperature in the presence of 5 mL of orange peel extract, which was added to the $AgNO_3$ solution without adjusting its pH. The reaction was allowed to reach completion as indicated by the golden brown color of the resulting AgNPs colloid solution. This
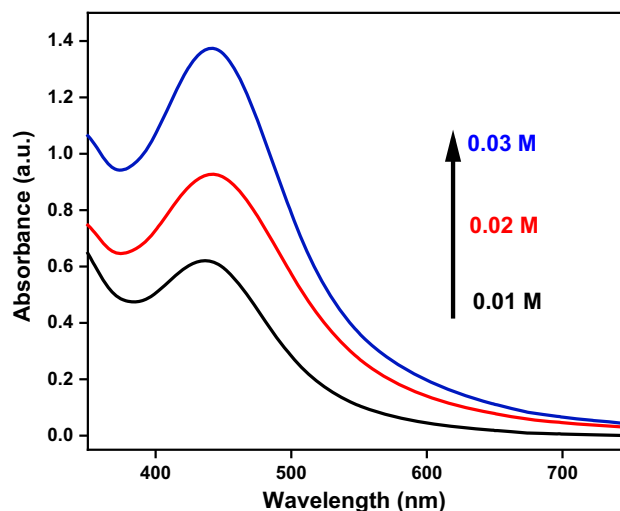

Fig. 1 UV–Vis absorbance spectra of AgNPs colloid solution synthesized with different concentrations of $AgNO_3$. Other factors are: volume of extract: 5 mL; temperature: room temperature; pH of extract: unadjusted natural pH; reaction time: until completed (golden brown color)

colloid solution exhibited an SPR absorption band at 420 nm and this band increased in intensity as the concentration of $AgNO_3$ rose from 0.01 to 0.03 M, suggesting the formation of more AgNPs with increasing concentration of silver ion [33]. This can be simply correlated to the Beer Lambert's Law ($A \propto C$), as the concentration of silver ions increased, the absorbance of the resulting AgNPs colloid solution increase proportionally, signifying a higher concentration of AgNPs in solution. A similar increase in SPR absorption band intensity with increasing silver ion concentration has been previously reported [34]. Very minor blue shifts (about 5 nm) may be discernible from the SPR absorption bands of AgNPs synthesized with 0.01–0.02 M $AgNO_3$ compared to that of 0.03 M (Fig. 1), such shifts may be ascribed to the formation of smaller sized silver nanoparticles at low concentration of silver ion [35].

3.2.2 Effect of Plant Extract Volume

Figure 2 shows the effect of extract volume on AgNPs synthesis. There was a variation observed in the SPR absorption bands on increasing the extract volume. When 3 mL of extract was used, a flat SPR absorption was observed and the golden brown color was not observed. This suggests that the natural antioxidants present in such extract volume are not sufficient to reduce the silver ions. An increase in volume of extract to 5 mL produced a marked difference as a highly intense absorbance was observed, suggesting that sufficient amounts of natural antioxidants associated with reducing the silver ions are now available in the 5 mL extract volume, which results in the formation of AgNPs. Such an effect of increase in absorbance with larger extract volume has been reported
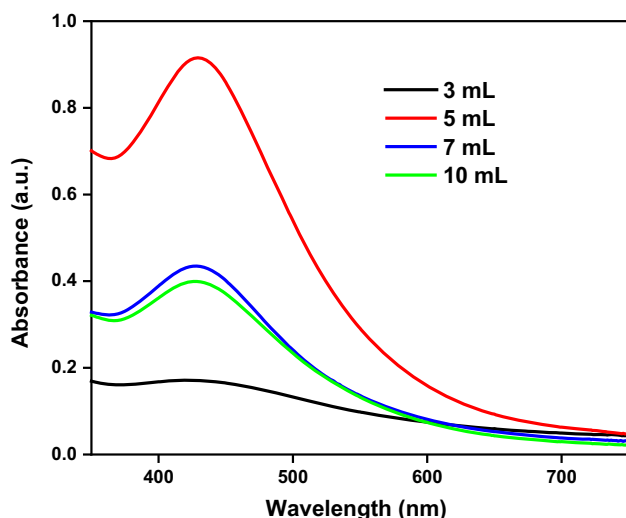
Fig. 2 UV–Vis absorbance spectra of AgNPs colloid solution synthesized with different volumes of orange peel extract. Other factors are: AgNO$_3$ concentration: 0.01 M, temperature: room temperature; pH of extract: unadjusted natural pH; reaction time: until completed (appearance of golden brown color)

previously [36, 37]. This result shows that an extract volume of 5 mL is sufficient to react with 40 mL of silver(I) ion solution, a volume ratio of 1:8. It also means that the amount of antioxidants present in an extract volume of 3 mL (1:13) is quite different from the optimal volume ratio required to initiate reduction of silver ion such that observable color changes characteristic of complete formation of AgNPs were not visible in a reasonable amount of time. As shown in Fig. 2, when 7 mL and 10 mL of orange peel extract were used, decrease in absorbance was observed. This can be ascribed to a change in volume ratio (1:6 and 1:4 instead of the optimal 1:8) and the dilution of the resulting colloidal solution, which was caused by an increase in extract volumes above the optimal volume of 5 mL mentioned above. This argument is consistent with the observation made in a previous publication on the green synthesis of gold nanoparticles, where a similar absorbance decrease was observed and ascribed to dilution of the colloidal solution [38].

3.2.3 Effect of pH

Another parameter studied was pH and the corresponding UV–Vis spectra obtained at different extract pHs are shown in Fig. S1. The pH of the orange peel extract was adjusted with dilute acid and base as required. Two separate sets of experiments were conducted, one in the acidic range (pH 3, 4, and 5) and the other in the alkaline range (pH 10, 11, and 12). Using the extract at the stated pHs, we observed that the formation of AgNPs was progressively faster as the pH becomes more alkaline. Hence, reactions conducted in alkaline pH of 12 took about 3 min while the ones conducted

under acidic conditions took about 15 min to complete. At pH 3, the observed SPR absorption band was weak and a light yellow color was detected. As the pH increased to 4 and 5, the SPR absorption bands became more intense and the colors deepened to golden brown (data not shown). The differences in colors have to do with variations in the pKa values of functional groups of the natural antioxidants such as flavonoids, and tannins that participate in the reduction of silver ion [39]. Generally, it has been established that alkalinity supports the bioreduction of silver and the subsequent formation of AgNPs in aqueous medium, this helps to explain the rapidity of the reactions in alkaline pHs and the relative slowness in acidic medium. It also accounts for the intensity of the SPR absorption bands, which increased as the pH increased [40]. Alkalinity is known to induce an electrostatic repulsion force among nanoparticles, thereby, effectively preventing them from agglomerating [37]. Also, the occurrence of surface plasmon resonance is favored in an alkaline medium [41]. On the other hand, acidity confers a very high-positive charge on the natural antioxidants (citric acid, hesperidin, and alkaloids) responsible for reducing silver ions, thus upon the formation of the nanoparticles, their stability will be low such that agglomeration will eventually occur [42].

3.2.4 Effect of Reaction Time

The synthesis of AgNPs was tracked with UV–Vis absorbance and the spectra recorded at time intervals of 2, 5, 10, 20, 40, and 80 min showed systematic increase in absorbance as the incubation or reaction time increased (Fig. 3). The bands formed at 2, 5, 10, and 20 min were within the range of 420–440 nm while those taken at 40 and 80 min showed a gradual shift below 420 nm. This infers a steady decrease in AgNPs size over time and similar trend has been previously reported [43]. The increase in absorbance with increasing incubation time could be attributed to an increase in the quantity of silver nanoparticles as the reaction progresses. There were concerns that as the incubation time increases, there is a big tendency for agglomeration of AgNPs, thereby, leading to the formation of bigger sized particles. However, our results here show that the as-synthesized AgNPs were highly stable and only a minimal agglomeration was observed even after 24 h (data not shown). The reaction times recorded in this study are significantly shorter than the 240 min and 24 h reported previously for AgNPs synthesis using Basil leaf and banana peel extract [43, 44]. The rapid synthesis of AgNPs recorded in this work is due to the excellent reduction potential of the active biocomponents and antioxidants present in the orange peel extract. Such natural antioxidants that actively participate in the nucleation, reduction, and stabilization of AgNPs include flavonoids, polyphenols, and citric acid. Flavonoids facilitate the reduc-
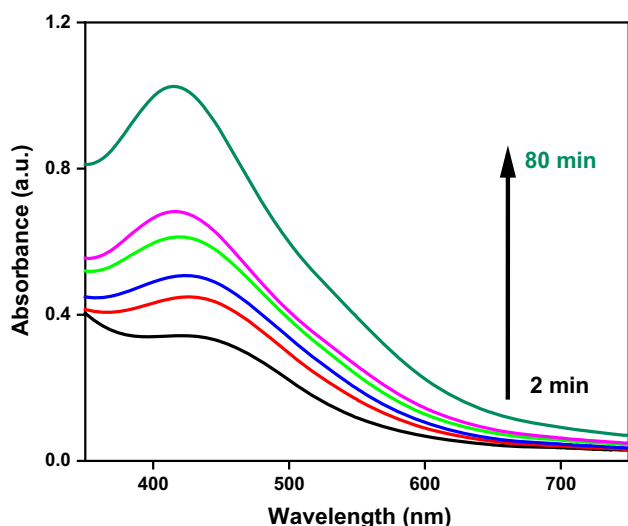
Fig. 3 UV–Vis absorbance spectra of AgNPs colloid solution taken from reaction vessel at different times. Other factors are: AgNO₃ concentration: 0.01 M, volume of extract: 5 mL; temperature: room temperature; pH of extract: unadjusted natural pH

tion of silver ions to nanoparticles by the tautomerization of their functional groups from enol to keto form while citric acid acts both as reducing and capping agents in AgNPs formation [45–47].

3.2.5 Effect of Temperature

The synthesis of silver nanoparticles varies greatly with temperature. The observed SPR absorption band (Fig. S2) for reactions conducted at various temperatures shows increase in absorption intensity as temperature increases. The working temperature under which the synthesis of AgNPs was conducted showed significant influence on the synthesis of AgNPs. At a lower temperature (25 °C), the reaction took 7 min to produce a color change and the SPR absorption was less intense (Fig. S2). However, as the temperature increased to 80 °C, the reduction of silver ion went faster; a change in color was noticed within 2 min and the SPR absorption became much more pronounced. Temperature is a critical factor in the synthesis of AgNPs and it accelerates the rate of the synthesis reaction by inducing rapid reduction of Ag^+ ions into AgNPs. Previous reports have shown that an increase in temperature leads to a decrease in the size of silver nanoparticles [48]. This is explained by the fact that as the temperature increases, the reaction proceeds more rapidly which leads to the homogenous nucleation of silver nuclei thereby leading to the formation of small-sized silver nanoparticles [49].

3.3 Optimum Conditions for AgNPs

After the study of physical parameters, a set of working conditions was selected as optimum reaction conditions that produced good yield of AgNPs in reasonable time (4 min) as determined from the absorbance maximum of the UV–Vis spectra obtained from the study of the physical parameters (see Figs. 1, 2, 3, and S1-S2). These optimum conditions were then used to synthesize the AgNPs that was used for characterization and colorimetric studies. These optimum conditions are: AgNO₃ concentration of 0.01 M, 1:8 volume ratio of orange peel extract to silver ion (5 mL and 40 mL, respectively), a temperature of 50 °C, a pH of 10; and a reaction time of 4 min. It must however be pointed out here that the actual visual color change (golden brown) that signifies complete AgNPs synthesis was almost instantaneous (less than min) under the optimum conditions, but we stopped the reaction at 4 min. Thus, orange peel extract with these optimum conditions produced AgNPs in less than 1 min. To our knowledge, this is the fastest procedure so far reported for green synthesis of AgNPs. So, the novelty of the current study lies in this record synthesis time, which can be adopted by other researchers as a 1-min synthesis method for producing AgNPs.

3.4 Silver Nanoparticles Characterization

The above-mentioned optimum conditions, which produce AgNPs in a record time of less than 1 min, were used to produce large quantities of the nanoparticles as stated in Sect. 2. The characterization of the resulting AgNPs was then conducted in order to determine their size, surface morphology, distribution, functional groups, and crystallinity. The results obtained provided an insight into the characteristics of the synthesized AgNPs.

3.4.1 Field Emission Scanning Electron Microscopy (FESEM) of AgNPs

A scanning electron microscope was used to determine the surface morphology and distributions of the AgNPs synthesized. FESEM image taken at 16,000 and 30,000 magnifications showed an array of polydisperse AgNPs (Fig. 4). From the image it is apparent that the nanoparticles have mostly amalgamated into nanoclusters. This might have occurred as a result of the longer incubation period the nanoparticles went through, as the incubation and drying protocols took about 18 h. It might also have arisen from the sample preparation method used for the FESEM analysis (see Sect. 2). The nanoparticles are mostly irregular in shape and their average size was estimated to be about 55 nm. The morphology of the AgNPs was found to be poorly defined and irregular. Barros et al. [6] has reported a similar obser-
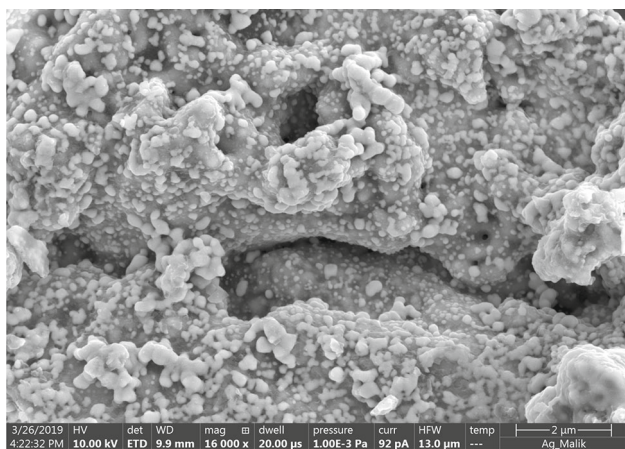
Fig. 4 FESEM image of orange peel extract-mediated synthesized AgNPs

vation with biosynthesized silver nanoparticles and ascribed the poorly defined morphology to the numerous reduction routes that silver ions may follow in a complex solution that contains multiple reducing agents like citric acid, flavonoids, and hesperidin.

3.4.2 Fourier Transform Infrared Spectroscopy (FTIR) Characterization

The FTIR spectrum obtained from the AgNPs is presented in Fig. S3. The spectrum shows that the AgNPs may be functionalized with biomolecules containing $-NH_2$, carbonyl and $-OH$ groups. The broad peak at 3433 cm^{-1} can be due to either O–H or N–H stretching vibrations from hydroxyl and amine groups of the extract constituents. Furthermore, the bands located at 2923 cm^{-1} and 2855 cm^{-1} were assigned to C–H stretching vibrations while the peak at 1629 cm^{-1} is due to either amide C=O stretching (proteins) or aromatic C–C stretching (flavonoids). The twin peaks occurring at 1459 cm^{-1} and 1380 cm^{-1} are within the range of amide III band and were assigned to N–H bending and C–N stretching of protein structures present in orange peel extract [34]. These results gave an insight into the functional groups involved in the synthesis reaction and they suggest that protein molecules in the extract may be involved in the stabilization of AgNPs through amide bonds [6].

3.4.3 X-ray Diffraction (XRD)

The XRD pattern of the AgNPs shown in Figure S4 obtained from X-ray diffraction analysis displayed three intense and sharp peaks and one less defined peak. The diffraction peaks obtained at 2θ angles of 37.11°, 40.86°, 67.05°, and 79.17° correspond to the 111, 200, 220, and 311 miller indices. The observed peaks point to the high crystallinity of the silver

nanoparticles and peaks arising from impurities were not detected. The narrowness of the peaks suggests a smaller sized silver nanocrystals. This is based on Scherrer's equation which states that the peak width is a major determinant of the size of nanoparticles crystallites [50]. The XRD patterns in Fig. S4 show good similarity with two different International Center for Diffraction Data (ICDD) files; 87-0717 and 87-0718 [51, 52]. According to the ICDD references, the orange peel-mediated AgNPs exhibit a face-centered cubic lattice structure.

3.5 Use of the Green AgNPs as a Colorimetric Nanosensor

3.5.1 Colorimetric Detection of Hg^{2+} ion by AgNPs

The colorimetric detection of mercury(II) ions using the synthesized AgNPs revealed a marked difference in UV–Vis absorbance response and visual color of the colloid solution after the addition of aqueous solution of Hg^{2+} ions. These ions caused a sudden change in the color of AgNPs colloid solution from golden brown to light brown and finally to colorless within 3 min of adding the Hg^{2+} solution (Fig. 5). This detection time of 3 min is about two times faster than that of a similar colorimetric sensor [17], and ten times faster than nanocomposite sensors [23–25]. The SPR absorption band of the AgNPs colloid solution also disappeared after adding Hg^{2+} ions as shown in Fig. S5. This suggests that the AgNPs can be used for visual colorimetric detection of Hg^{2+} ions in water. However, when other cations (Na^{2+}, Ca^{2+}, Mg^{2+}, Al^{3+}, Cd^{2+}, Ni^{2+}) were added to the AgNPs colloid solution, there was no such dramatic change in color and there was no disappearance of the SPR absorption band of the colloid solution (Figs. 5 and S5). This suggests that the observed changes are specific to a peculiar interaction between mercury and nanoscale silver. Thus, the AgNPs are selective toward Hg^{2+} ions and show no dramatic changes toward other cations tested. It may be inferred that the selectivity of AgNPs toward mercury(II) ions is built upon its ability to form silver–mercury amalgam [17]; other metallic cations do not form amalgams with silver and so they do not cause a significant change in color or loss of SPR absorption band when they interact with AgNPs [29].

The mechanism of silver–mercury amalgam formation has been previously described by Rastogi et al. [17], and it has been established that physical and chemical properties of nanoscale metal particles are different from those of bulk metal [53, 54]. The difference in the standard electrode potential of silver (Ag^+/Ag: $E^0 = 0.79$ V) and that of mercury (Hg^{2+}/Hg: $E^0 = 0.85$ V) is very small and is therefore not expected to favor a fast redox reaction between Hg^{2+} and Ag^0 [17]. In the same vein, the Ag^+/Ag_{nano} redox potential for AgNPs is quite different from that of Ag^+/Ag_{Metal}
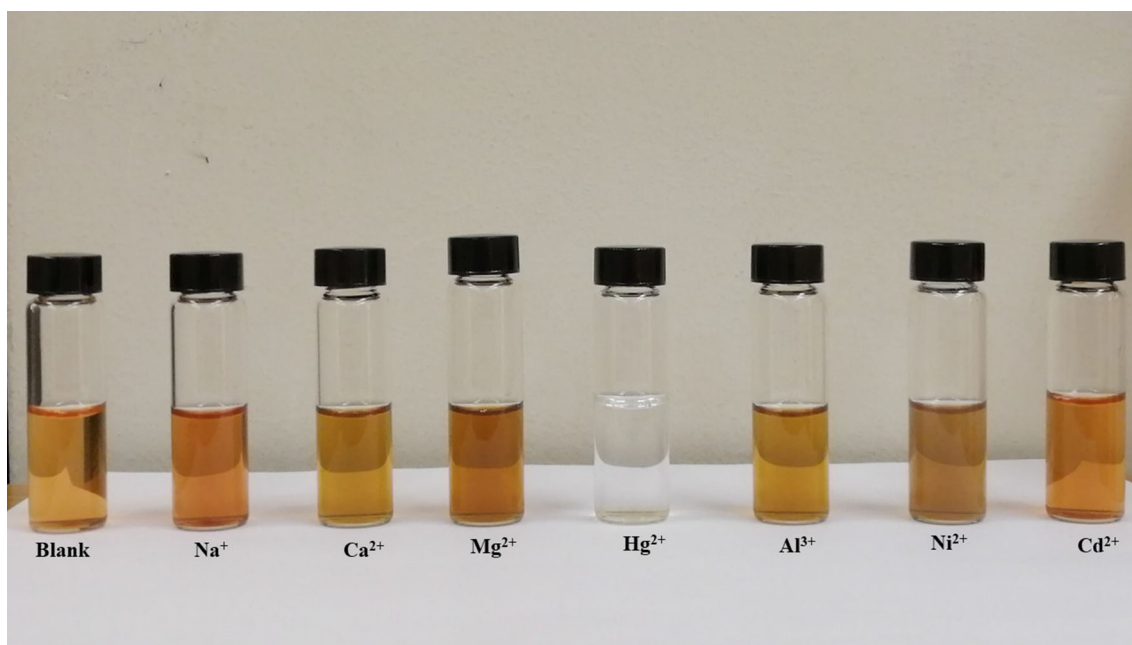
Fig. 5 Picture showing the color change observed after adding various metal ions to the AgNPs colloid solution. As explained in the text, only Hg^{2+} solution gave a complete disappearance of the golden brown color of the colloid solution. Other metal ions did not show such a dramatic change in color

in the bulk metal. Thus, there is a progressive decrease in the redox potential as the size of the metal particle progressively decreases into the nanoscale, which therefore widens the potential difference between Ag^+/Ag_{nano} and Hg^{2+}/Hg and favors reduction of Hg^{2+} to Hg with partial oxidation of Ag_{nano} [17, 55]. The strong affinity between silver and mercury leads to the deposition of mercury onto the silver surfaces thereby leading to the formation of silver–mercury amalgam [56], which is responsible for the significant decrease in SPR absorption intensity and of course the disappearance of the golden brown color of AgNPs colloidal solution [17] as shown in Fig. 5. Therefore, the observed dramatic change in color of AgNPs colloid solution upon addition of Hg^{2+} stems from the formation of silver–mercury amalgam, which is made possible by the nanoscale size of the silver and the strong affinity between silver and mercury.

The dramatic visual color change observed on adding aqueous solution of Hg^{2+} ions to the AgNPs colloid solution, which also showed up as a complete disappearance of the SPR absorption band (Figs. 5 and S5) was quantified as shown in Fig. 6. The net absorbance was plotted for all the metal ions tested, including Hg^{2+} ions. Net absorbance is given by:

$$\text{Net absorbance} = A_{AgNPs} - A_M^{n+}$$

where A_{AgNPs} is the absorbance of the AgNPs colloid solution before adding a metal ion and A_M^{n+} is the absorbance of the AgNPs colloid solution after adding a metal ion. Figure 6
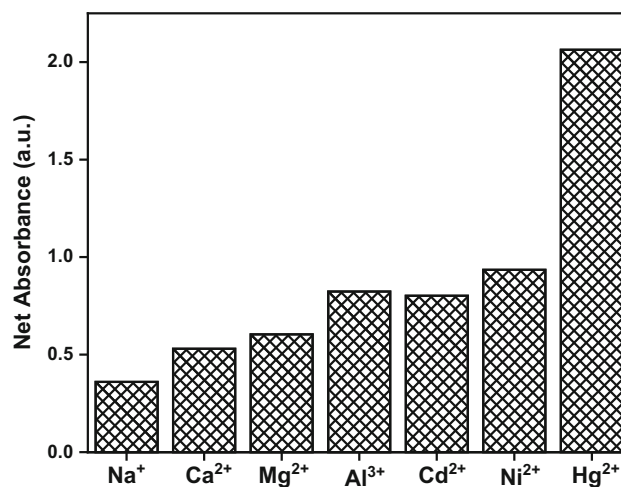

Fig. 6 Net absorbance recorded for different metals. Hg^{2+} gave the highest net absorbance

shows that the largest net absorbance was observed for Hg^{2+} ions and as shown in Fig. S5, there was a complete loss of SPR absorption band with the addition of Hg^{2+} ion, which led to a flat absorbance response.

3.5.2 Sensitivity of the AgNPs Sensor for Hg^{2+} Ion

In establishing the sensitivity of synthesized AgNPs toward Hg^{2+} ion, the concentration of this cation was varied from 1 to 100 μM as shown in Fig. 7. We observed that with
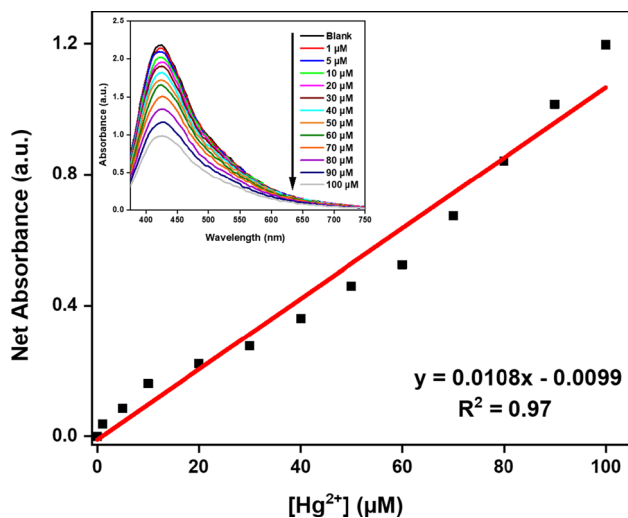
Fig. 7 Concentration-dependent plot of net absorbance versus Hg^{2+} concentration. Increasing Hg^{2+} concentration gives linearly increasing net absorbance values. The corresponding absorption spectra are shown in the inset
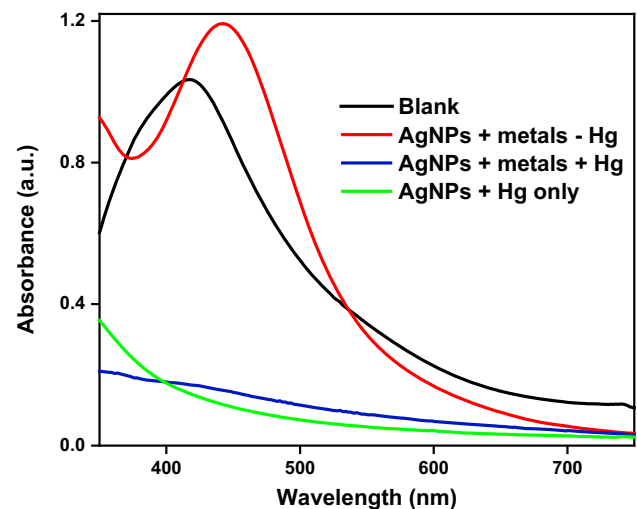

Fig. 8 UV–Vis absorbance spectra of AgNPs colloid solution in the presence of a mixture of metal ions to show that the presence of other metal ions does not pose interference in the colorimetric detection of Hg^{2+}

every increase in the concentration of Hg^{2+}, the UV spectra showed progressive loss of absorbance intensity and the color intensity of the solution visually diminished as well. The variation in concentration was found to produce a linear response within the range of 1–100 μM tested (Fig. 7), with a limit of detection (LOD) of 1.25×10^{-6} M (0.25 ppm). This LOD value is similar to LOD values previously reported for Hg^{2+} ion using AgNPs [29, 30], but this value is not as good as the LOD values reported earlier with nanocomposite and mesoporous sensors and adsorbents [23–25].

3.5.3 Selectivity of the AgNPs Sensor for Hg^{2+} Ion in the Presence of Other Metal Ions

We also tested the robustness of this colorimetric Hg^{2+} detection method to possible interferences in samples that may contain various metals in a single medium. To this end, a complex mix of different metal ions was prepared in order to test the possibility of interferences from other metal ions. Equal volumes (1 mL) each of 1 mM solutions of Na^{2+}, Ca^{2+}, Mg^{2+}, Al^{3+}, Cd^{2+}, Ni^{2+} and Hg^{2+} were mixed together and added to 1 mL of AgNPs colloid solution. Another solution was made in which all these metal ions were mixed with the exception of Hg^{2+} and added to 1 mL of AgNPs colloid solution. A third solution containing only Hg^{2+} was also prepared and similarly added to AgNPs colloid solution. Figure 8 presents the corresponding UV–Vis spectra for all the three solutions. It is clear from the figure that the presence of other metals did not present significant interference on the ability of AgNPs to selectively detect Hg^{2+} ions. Thus, the colorimetric detection of Hg^{2+} by AgNPs suffers little or no interference from other metal ions. For the solution containing all the metal ions except Hg^{2+} the SPR absorption band was intact. However, inclusion of Hg^{2+} in the mixture led to the disappearance of the band (Fig. 8).

3.5.4 Detection of Hg^{2+} Ion in Drinking Water

In addition to the above studies, we tested this visual colorimetric detection method with drinking water. Initial colorimetric test revealed that the water sample did not contain detectable amounts of mercury, so we spiked the water with 4 mL of 20, 40, 60, and 80 μM Hg^{2+} (Fig. S6). The recorded absorbance versus concentration as shown in Fig. S6 is linear. This shows that the orange peel-mediated synthesized AgNPs could be deployed for colorimetric test for mercury ions in drinking water.

4 Conclusion

A simple, cost-effective, environmental-friendly and green synthesis of AgNPs using orange peel extract is presented in this work. The one-pot synthesis employed is based on the concept of green chemistry and it sidestepped the use of toxic chemicals such as reducing agents, surfactants and stabilizers. The physicochemical parameters that influence the formation of the nanoparticles were investigated, which enabled us to select a set of optimum conditions for AgNPs synthesis. These optimum conditions produced AgNPs within 1 min, which is a record time ever reported for green AgNPs synthesis. We characterized the resulting AgNPs to determine their size, crystallinity, surface morphology and surface chemistry using various techniques.

FTIR results showed spectral signatures characteristic of the natural antioxidants that may be actively involved in the reduction of silver nitrate to AgNPs. The XRD pattern observed revealed that the silver nanoparticles possess crystalline face-centered cubic (fcc) lattice structures and the data are in good agreement with ICDD XRD database. FESEM images showed polydisperse silver nanoparticles of irregular shape and poorly defined morphology. The as-synthesized AgNPs were utilized for visual colorimetric detection of Hg^{2+} ions in water and we found the AgNPs to be both sensitive and selective toward Hg^{2+} ions, giving a detection limit of 0.25 ppm. Therefore, the detection limit and sensitivity recorded for Hg^{2+} ions in the present work is comparable to what have been previously reported for Hg^{2+} detection using AgNPs sensors, it is not as low as the detection limits reported with nanocomposite and mesoporous sensors and adsorbents. However, the actual colorimetric detection of Hg^{2+} with the new AgNPs sensor is much faster than several other similar colorimetric methods. The AgNPs are also of low cost, non-toxic and biocompatible, while they show good selectivity and colloidal stability. On the overall, the current work adds to the repertoire of simple, one-pot AgNPs synthesis methods available, and the 1-min synthesis protocol presented can be employed by other researchers as a very fast AgNPs synthesis method.

References

1. Annadhasan, M.; Muthukumarasamyvel, T.; Sankar Babu, V.R.; Rajendiran, N.: Green synthesized silver and gold nanoparticles for colorimetric detection of Hg^{2+}, Pb^{2+}, and Mn^{2+} in aqueous medium. ACS Sustain. Chem. Eng. **2**, 887–896 (2014)
2. Mohamed, M.B.; Volkov, V.; Link, S.; El-Sayed, M.A.: The 'lightning' gold nanorods: fluorescence enhancement of over a million compared to the gold metal. Chem. Phys. Lett. **317**, 517–523 (2000)
3. Rai, M.; Gade, A.; Yadav, A.: Biogenic nanoparticles: an introduction to what they re, how they are synthesized and their applications in microbiology. In: Rai, M., Duran, N. (eds.) Metal Nanoparticles in Microbiology, pp. 1–14. Springer, Berlin (2011)
4. Saxena, A.; Tripathi, R.M.; Zafar, F.; Singh, P.: Green synthesis of silver nanoparticles using aqueous solution of *Ficus benghalensis* leaf extract and characterization of their antibacterial activity. Mater. Lett. **67**, 91–94 (2012)
5. Yunus, I.S.; Harwin,; Kurniawan, A.; Adityawarman, D.; Indarto, A.: Nanotechnologies in water and air pollution treatment. Environ. Technol. Rev. **1**, 136–148 (2012)
6. de Barros, C.H.N.; Cruz, G.C.F.; Mayrink, W.; Tasic, L.: Bio-based synthesis of silver nanoparticles from orange waste: effects of distinct biomolecule coatings on size, morphology, and antimicrobial activity. Nanotechnol. Sci. Appl. **11**, 1–14 (2018)
7. Hemlata,; Meena, P.R.; Singh, A.P.; Tejavath, K.K.: Biosynthesis of silver nanoparticles using *Cucumis prophetarum* aqueous leaf extract and their antibacterial and antiproliferative activity against cancer cell lines. ACS Omega **5**, 5520–5528 (2020)
8. Akhtar, M.S.; Panwar, J.; Yun, Y.-S.: Biogenic synthesis of metallic nanoparticles by plant extracts. ACS Sustain. Chem. Eng. **1**, 591–602 (2013)
9. Park, Y.: A new paradigm shift for the green synthesis of antibacterial silver nanoparticles utilizing plant extract. Toxicol. Res. **30**, 169–178 (2014)
10. Hembram, K.C.; Kumar, R.; Kandha, L.; Parhi, P.K.; Kundu, C.N.; Bindhani, B.K.: Therapeutic prospective of plant induced silver nanoparticles application as antimicrobial and anticancer agent. Artif. Cells Nanomed. Biotechnol. **46**, S38–S51 (2018)
11. Zahir, F.; Rizwi, S.J.; Haq, S.K.; Khan, R.H.: Low dose mercury toxicity and human health. Environ. Toxicol. Pharmacol. **20**, 351–360 (2005)
12. Holmes, P.; James, K.A.; Levy, L.S.: Is low-level environmental mercury exposure of concern to human health? Sci. Total Environ. **408**, 171–182 (2009)
13. Yamini, Y.; Alizadeh, N.; Shamsipur, M.: Solid phase extraction and determination of ultra trace amounts of mercury(II) using octadecyl silica membrane disks modified by hexathia-18-crown-6-tetraone and cold vapour atomic absorption spectrometry. Anal. Chim. Acta **355**, 69–74 (1997)
14. Kuswandi, B.; Nuriman, A.; Dam, H.H.; Reinhoudt, D.N.; Verboom, W.: Development of a disposable mercury ion-selective optode based on trityl-picolamide as ionophore. Anal. Chim. Acta **591**, 208–213 (2007)
15. Fong, B.S.; Siu, T.S.; Lee, J.S.; Tam, S.: Determination of mercury in whole blood and urine by inductively coupled plasma mass spectrometry. J. Anal. Toxicol. **31**, 281–287 (2007)
16. Ichinoki, S.; Kitahata, N.; Fujii, Y.: Selective determination of mercury(II) ion in water by solvent extraction followed by reversed-phase HPLC. J. Liq. Chromatogr. Relat. Technol. **27**, 1785–1798 (2004)
17. Rastogi, L.; Sashidhar, R.B.; Karunasagar, D.; Arunachalam, J.: Gum kondagogu reduced/stabilized silver nanoparticles as direct colorimetric sensor for the sensitive detection of Hg^{2+} in aqueous system. Talanta **118**, 111–117 (2014)
18. Stewart, M.E.; Anderton, C.R.; Thompson, L.B.; Maria, J.; Gray, S.K.; Rogers, J.A.; Nuzzo, R.G.: Nanostructured plasmonic sensors. Chem. Rev. **108**, 494–521 (2008)
19. Yang, Y.-K.; Yook, K.-J.; Tae, J.: A rhodamine-based fluorescent and colorimetric chemodosimeter for the rapid detection of Hg^{2+} ions in aqueous media. J. Am. Chem. Soc. **127**, 16760–16761 (2005)
20. Zhu, Z.; Su, Y.; Li, J.; Li, D.; Zhang, J.; Song, S.; Zhao, Y.; Li, G.; Fan, C.: Highly sensitive electrochemical sensor for mercury(II) ions by using a mercury-specific oligonucleotide probe and gold nanoparticle-based amplification. Anal. Chem. **81**, 7660–7666 (2009)
21. Liu, J.; Lu, Y.: Rational design of turn-on allosteric DNAzyme catalytic beacons for aqueous mercury ions with ultrahigh sensitivity and selectivity. Angew. Chem. Int. Ed. **46**, 7587–7590 (2007)
22. Lu, H.; Tang, Y.; Xu, W.; Zhang, D.; Wang, S.; Zhu, D.: Highly selective fluorescence detection for mercury(II) ions in aqueous solution using water soluble conjugated polyelectrolytes. Macromol. Rapid Commun. **29**, 1467–1471 (2008)
23. Awual, M.R.; Hasan, M.M.; Eldesoky, G.E.; Khaleque, M.A.; Rahman, M.M.; Naushad, M.: Facile mercury detection and removal from aqueous media involving ligand impregnated conjugate nanomaterials. Chem. Eng. J. **290**, 243–251 (2016)
24. Abbas, K.; Znad, H.; Awual, M.R.: A ligand anchored conjugate adsorbent for effective mercury(II) detection and removal from aqueous media. Chem. Eng. J. **334**, 432–443 (2018)

25. Awual, M.R.: Novel nanocomposite materials for efficient and selective mercury ions capturing from wastewater. Chem. Eng. J. **307**, 456–465 (2017)

26. Awual, M.R.: An efficient composite material for selective lead(II) monitoring and removal from wastewater. J. Environ. Chem. Eng. **7**, 103807 (2019)

27. Awual, M.R.: A facile composite material for enhanced cadmium(II) ion capturing from wastewater. J. Environ. Chem. Eng. **7**, 103378 (2019)

28. Awual, M.R.; Hasan, M.M.: A ligand based innovative composite material for selective lead(II) capturing from wastewater. J. Mol. Liq. **294**, 111679 (2019)

29. Farhadi, F.; Forough, M.; Molaei, R.; Hajizadeh, S.; Rafipour, A.: Highly selective Hg^{2+} colorimetric sensor using green synthesized and unmodified silver nanoparticles. Sens. Actuators B. Chem. **161**, 880–885 (2012)

30. Bothra, S.; Solanki, J.N.; Sahoo, S.K.: Functionalized silver nanoparticles as chemosensor for pH, Hg^{2+} and Fe^{3+} in aqueous medium. Sens. Actuators B. Chem. **188**, 937–943 (2013)

31. Park, J.; Joo, J.; Kwon, S.G.; Jang, Y.; Hyeon, T.: Synthesis of monodisperse spherical nanocrystals. Angew. Chem. Int. Ed. **46**, 4630–4660 (2007)

32. Khatoon, N.; Mazumder, J.A.; Sardar, M.: Biotechnological applications of green synthesized silver nanoparticles. J. Nanosci. Curr. Res. **2**, 1000107 (2017)

33. Zaki, S.; El Kady, M.F.; Abd-El-Haleem, D.: Determination of the effective origin source for nanosilver particles produced by *Escherichia coli* strain S78 and its application as antimicrobial agent. Mater. Res. Bull. **47**, 4286–4290 (2012)

34. Dubey, S.P.; Lahtinen, M.; Sillanpaa, M.: Tansy fruit mediated greener synthesis of silver and gold nanoparticles. Process Biochem. **45**, 1065–1071 (2010)

35. Mock, J.J.; Barbic, M.; Smith, D.R.; Schultz, D.A.; Schultz, S.: Shape effects in plasmon resonance of individual colloidal silver nanoparticles. J. Chem. Phys. **116**, 6755–6759 (2002)

36. Huang, J.; Li, Q.; Sun, D.; Lu, Y.; Su, Y.; Yang, X.; Wang, H.; Wang, Y.; Shao, W.; He, N.: Biosynthesis of silver and gold nanoparticles by novel sundried *Cinnamomum camphora* leaf. Nanotechnology **18**, 105104 (2007)

37. Sathishkumar, M.; Sneha, K.; Yun, Y.-S.: Palladium nanocrystals synthesis using *Curcuma longa* tuber extract. Int. J. Mater. Sci. **4**, 11–17 (2009)

38. Noruzi, M.; Zare, D.; Khoshnevisan, K.; Davoodi, D.: Rapid green synthesis of gold nanoparticles using *Rosa hybrida* petal extract at room temperature. Spectrochim. Acta A **79**, 1461–1465 (2011)

39. Pimprikar, P.S.; Joshi, S.S.; Kumar, A.R.; Zinjarde, S.S.; Kulkarni, S.K.: Influence of biomass and gold salt concentration on nanoparticle synthesis by the tropical marine yeast *Yarrowia lipolytica*. Colloids Surf. B Biointerfaces **74**, 309–316 (2009)

40. Alqadi, M.K.; Abo Noqtah, O.A.; Alzoubi, F.Y.; Alzouby, J.; Aljarrah, K.: pH effect on the aggregation of silver nanoparticles synthesized by chemical reduction. Mater. Sci. Pol. **32**, 107–111 (2014)

41. Vanaja, M.; Annadurai, G.: *Coleus aromaticus* leaf extract mediated synthesis of silver nanoparticles and its bactericidal activity. Appl. Nanosci. **3**, 217–223 (2012)

42. Khalil, M.M.H.; Ismail, E.H.; El-Baghdady, K.Z.; Mohamed, D.: Green synthesis of silver nanoparticles using olive leaf extract and its antibacterial activity. Arab. J. Chem. **7**, 1131–1139 (2014)

43. Salawu, O.A.; Chanbasha, B.; Zafarullah, K.; Alsharaa, A.; Siddiqui, Z.: Biogenic synthesis of silver nanoparticles, study of the effect of physicochemical parameters and application as nanosensor in the colorimetric detection of Hg^{2+} in water. Int. J. Environ. Anal. Chem. **96**, 776–788 (2016)

44. Ibrahim, H.M.M.: Green synthesis and characterization of silver nanoparticles using banana peel extract and their antimicrobial activity against representative microorganisms. J. Radiat. Res. Appl. Sci. **8**, 265–275 (2015)

45. Makarov, V.V.; Love, A.J.; Sinitsyna, O.V.; Makarova, S.S.; Yaminsky, I.V.; Taliansky, M.E.; Kalinina, N.O.: "Green" nanotechnologies: synthesis of metal nanoparticles using plants. Acta Nat. **6**, 35–44 (2014)

46. Ahmad, N.; Sharma, S.; Alam, M.K.; Singh, V.N.; Shamsi, S.F.; Mehta, B.R.; Fatma, A.: Rapid synthesis of silver nanoparticles using dried medicinal plant of basil. Colloids Surf. B Biointerfaces **81**, 81–86 (2010)

47. Prathna, T.C.; Chandrasekaran, N.; Raichur, A.M.; Mukherjee, A.: Biomimetic synthesis of silver nanoparticles by *Citrus limon* (lemon) aqueous extract and theoretical prediction of particle size. Colloids Surf. B Biointerfaces **82**, 152–159 (2011)

48. Fayaz, A.M.; Balaji, K.; Kalaichelvan, P.T.; Venkatesan, R.: Fungal based synthesis of silver nanoparticles-an effect of temperature on the size of particles. Colloids Surf B Biointerfaces **74**, 123–126 (2009)

49. Jiang, J.; Manolache, S.; Lee Wong, A.C.; Denes, F.S.: Plasma enhanced deposition of silver nanoparticles onto polymer and metal surfaces for the generation of antimicrobial characteristics. J. Appl. Polym. Sci. **93**, 1411–1422 (2004)

50. Peterson, A.L.: The Scherrer formula for X-ray particle size determination. Phys. Rev. **56**, 978–982 (1939)

51. Gopinath, V.; MubarakAli, M.; Priyadarshini, S.; Priyadharsshini, N.M.; Thajudin, N.; Velusamy, P.: Biosynthesis of silver nanoparticles from *Tribulus terrestris* and its antimicrobial activity: a novel biological approach. Colloid Surf. B Biointerfaces **96**, 69–74 (2012)

52. Dhand, V.; Soumya, L.; Bharadwaj, S.; Chakra, S.; Deepika, B.; Sreedhar, B.: Green synthesis of silver nanoparticles using *Coffea arabica* seed extract and its antibacterial activity. Mater. Sci. Eng. C **58**, 36–43 (2016)

53. Henglein, A.: Small-particle research: physicochemical properties of extremely small colloidal metal and semiconductor particles. Chem. Rev. **89**, 1861–1873 (1989)

54. de Cointet, C.; Mostafavi, M.; Khatouri, J.; Belloni, J.: Growth and reactivity of silver clusters in cyanide solution. J. Phys. Chem. B **101**, 3512–3516 (1997)

55. Pradhan, N.; Pal, A.; Pal, T.: Silver nanoparticle catalyzed reduction of aromatic nitro compounds. Colloids Surf. A Physicochem. Eng. Asp. **196**, 247–257 (2002)

56. Lee, K.H.; Shin, M.C.; Lee, J.Y.: A kinetic study of the silver–mercury contact reaction. J. Mater. Sci. **21**, 2430–2434 (1986)